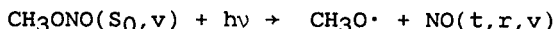# Photodissociation of molecules: the microscopic path of a molecular decay

J.Robert Huber

Physikalisch-Chemisches Institut der Universität Zürich,
Winterthurerstr. 190, CH-8057 Zürich, Switzerland

Abstract - The state-selective photodissociation of methylnitrite

$$CH_3ONO(S_0,v) + h\nu \rightarrow CH_3O\cdot + NO(t,r,v)$$

is reviewed and the dynamics of the bond-breaking process is analysed
in connection with an ab initio $S_1$-potential energy surface of the
parent molecule. Experimental and theoretical results reveal an in-
teresting picture of the dissociation path of a polyatomic molecule
which decays by vibrational predissociation and a strong exit channel
interaction.

## INTRODUCTION

If a polyatomic molecule absorbs light with an energy exceeding the disso-
ciation energy of its weakest bond, fragmentation can occur which produces
products in excited states. The dynamics of the process, which in turn is
given by the potential energy surface of the excited parent molecule, deter-
mines the fragmentation pathway and energy distribution in the photoproducts
(ref. 1). According to the dissociation dynamics we may distinguish between
a **direct dissociation** and a **predissociation**. In the case of a direct disso-
ciation the excited state potential energy surface (PES) is antibonding and
strongly repulsive along one or more coordinates yielding an extremly fast
( < 10 fs) bond-breaking process (cf. Fig. 1a). The absorption spectrum of
the parent molecule is, therefore, broad and structureless. Predissociation,
on the other hand, may be the result of an excited state PES characterized
by a local well along the reaction coordinate as depicted in Fig. 1b.
The potential well can support quasi-bound levels of the excited molecule
and due to the barrier, the decay of the excited molecule is slow compared
to direct dissociation (~ 100 fs). The decay is induced either by tunneling
through the barrier in the case of an adiabatic process, and/or by coupling
between internal and dissociative modes in the case of a nonadiabatic proc-
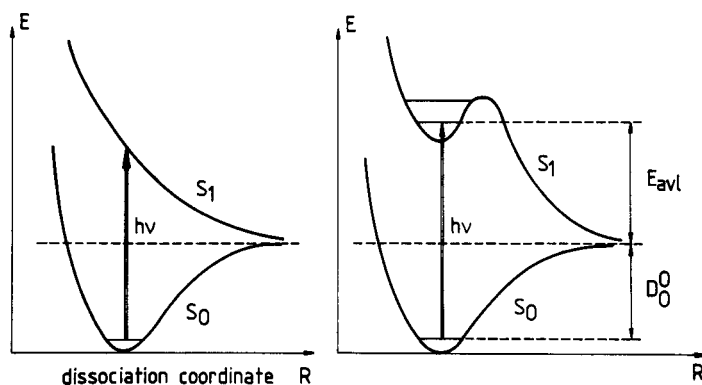ess. The potential well acts like a short-term waiting room for the excited



Fig. 1.    Direct dissociation, left (a) and
indirect dissociation (predissociation), right (b)

molecule to decay and it gives rise to pronouced structures in the absorp-
tion spectrum which reflect the energy spacings of the quasi-bound states
supported by the potential well. Under these conditions the excitation proc-
ess and the decay of the excited complex can be treated separately (see
below).

In the present communication we will focus on predissociation, in particu-
lar, on the experimental and theoretical results obtained from a photodisso-
ciation study of methylnitrite excited into different vibrational levels of
the electronic state $S_1$ (refs. 2 - 11). It is shown that methylnitrite is an
example of **vibrational predissociation** and an excellent system to explore in
detail the microscopic decay path of an excited polyatomic molecule.

## POTENTIAL ENERGY SURFACE

The weak $S_1(n\pi^*) \leftarrow S_0$ transition of methylnitrite is localized in the O-N=O
moiety. Figure 2 shows the spectrum which is dominated by the absorption of
the cis-conformer of $CH_3ONO$. It is characterized by a well defined progres-
sion of the N=O stretching vibration $\nu_3 \sim 1000$ cm$^{-1}$. Excitation into a
vibronic level associated with $\nu_3$ ($S_1$, $n^*$) results in prompt dissociation
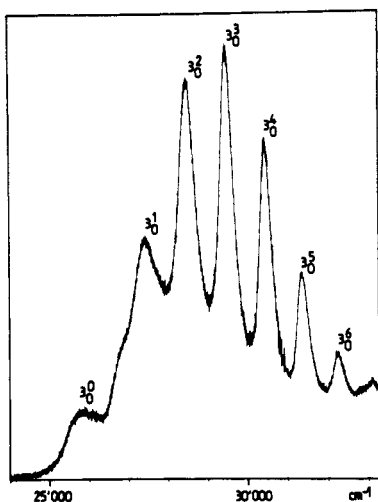producing NO and a methoxy radical (refs. 2 - 7).



Fig. 2. $S_1 \leftarrow S_0$ absorption spectrum of
$CH_3ONO$ in the gas phase at room tem-
perature. The $\nu_3$ progression is due to
the N=O stretching vibration. The
spectrum is dominated by the cis-form.

Owing to the localized nature of the $n\pi^*$ excitation, it was expected that a
two-dimensional PES involving the coordinates $r_{N=O}$ and $R_{O-N}$ could provide a
realistic description for the dissociation process. The result of an ab
initio (MCSCF) calculation (ref. 5) of such a two-dimensional $S_1$-PES for
cis-$CH_3ONO$ is given in Fig. 3. Two features of this PES are of importance.
First, a shallow well is evident along the dissociation coordinate $R_{O-N}$ and
close to the Franck-Condon region (excitation region) probably caused by an
avoided crossing with a higher state. If this well can support quasi-bound
energy levels, we encounter a situation very similar to the one described in
Fig. 1b. Second, the minimum energy dissociation path is strongly curved
which means that the potential parameters of the N=O group, namely the bond
length and the force constant, depend significantly on the $CH_3O$--NO separa-
tion. This fact indicates a strong vibrational-translational coupling that
is responsible for the redistribution of internal energy during the separa-
tion of the fragments and thus to a great extent to the final energy parti-
tioning (ref. 10). A very similar picture was found for the related molecule
HONO (refs. 12, 13).

Based on these findings the photodissociation can be treated as a two-step
process (ref. 10)

$$CH_3ONO(S_0|n=0) + h\nu \rightarrow CH_3ONO(S_1|n^*) \tag{1}$$

$$CH_3ONO(S_1|n^*) \rightarrow NO(t,v,r,e) + CH_3O(t,v,r) \tag{2}$$
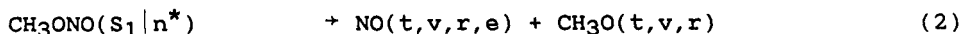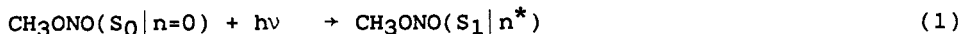
where n and $n^*$ denote the (effective) quantum numbers of $\nu_3$ in the $S_0$ and $S_1$
states, respectively.
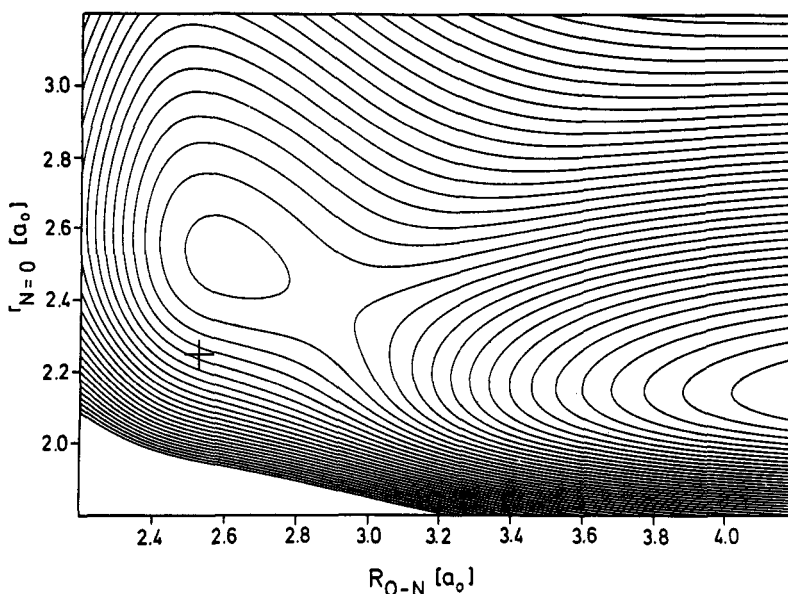
Fig. 3. Contour plot of the ab initio $S_1$-potential surface of $CH_3ONO$ (ref. 5). The energy spacing is 0.136 eV. The cross indicates the equilibrium of $S_0$ (Franck-Condon region).

## EXPERIMENTAL RESULTS

The photodissociation of $CH_3ONO$ was investigated after excitation into the $3_0^1$ (363.9 nm), $3_0^2$ (350.8 nm) and $3_0^3$ (338.4 nm) vibronic bands (cf. Fig. 2). The energy $E_{avl}$ which is available to be distributed among the internal degrees of freedom and the recoil of the NO and $CH_3O$ fragments is given by

$$E_{avl} = E_0(CH_3ONO) + h\nu - D_0^0 \qquad (3)$$

where $E_0(CH_3ONO) \sim 700$ cm$^{-1}$ is the internal energy of the parent, $h\nu$ the excitation energy, and $D_0^0 = 14500 \pm 400$ cm$^{-1}$ the dissociation energy of $CH_3O$-NO. For the three excitation wavelengths used we obtain $E_{avl} = 13750$, 14730 and 15770 cm$^{-1}$, respectively (refs. 3, 9).

We probed the internal energy distribution and the translational energy of the NO fragments emerging from the dissociation using an apparatus and methods described elsewhere (ref. 14). Briefly, two polarized laser beams, one to dissociate $CH_3ONO$ and one to probe NO, were crossed in a gas cell flowed continuously with $CH_3ONO$ at a pressure of $\sim$ 100 mTorr. The probe laser pulse was optically delayed by 10 ns relative to the dissociation laser pulse. In order to protect the parent molecule from the analyzing laser light, nascent $NO(X^2\Pi)$ was probed using two photon laser induced fluorescence (LIF) ($2x \sim$ 450 nm). Figure 4 shows the rotational spectrum of a single vibrational level of nascent NO taken 10 ns after the photodissociation of $CH_3ONO$. Such a spectrum measured under different polarization conditions for all populated
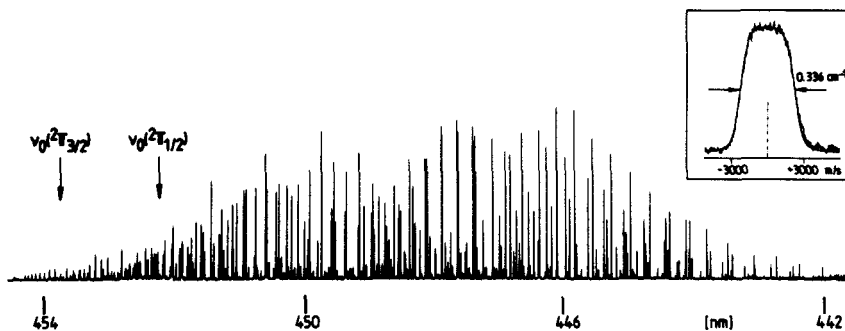


Fig. 4. Rotational (LIF) spectrum of nascent NO(v"=0) after photodissociation of $CH_3ONO$ at 363.9 nm. The insert shows the Doppler profile of a selected rotational line.

Fig. 5. Rotational state popu-
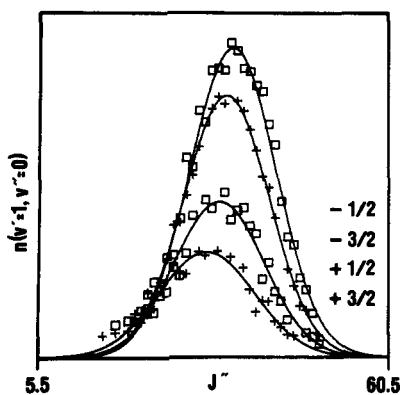lation distributions of the
four sublevels of NO(v"=0)
created in the photodisso-
ciation of $CH_3ONO$ ($S_1$, n=1).



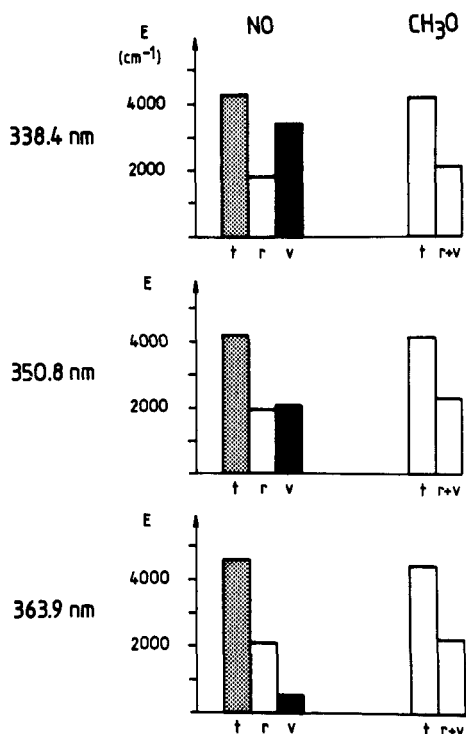Fig. 6. Energy partitioning (t=trans-
lational, v=vibrational, r=rotation-
al) into the NO and $CH_3O$ fragments
after photodissociation of $CH_3ONO$ at
three different excitation wave-
lengths ($3_0^1$, $3_0^2$, $3_0^3$).

vibrational states of NO contains the basic information of the internal
state distribution. From the intensities one obtains the state populations
and from the intensity variation for different probe laser polarizations,
the rotational alignment and hence, information about the geometry of the
dissociation process (ref. 15). Figure 5 shows the rotational state distri-
bution of nascent NO in its zeroth vibrational level. In the case of the NO
fragment, the spectrum can be disentangled into 4 rotational sub-spectra be-
longing to the two spin-levels 1/2 and 3/2 and their two Λ-sublevels ($\Pi_{\pm 1/2}$,
$\Pi_{\pm 3/2}$). These spectra provide further information about the energetics and
the geometry of the bond-breaking process (ref. 16).

Finally, the recoil velocity distribution and the translational energy of
the fragment are deduced from Doppler profile measurements shown as inserts
in Fig. 4. Furthermore, the Doppler profile analysis yields the parameter β
which is a measure of the spatial anisotropy of the fragment (ref. 17).
Since the degree of this anisotropy depends on the dissociation time $t_{diss}$
and the angular frequency of rotation of the excited parent molecule, the
parameter provides an upper limit of $t_{diss}$. Based on this fact, the excited
$CH_3ONO$ "complex" was found to dissociate within 200 fs (ref. 6).

Having determined the complete state distribution and the three-dimensional
recoil velocity distribution of NO, we also know the translational energy of
$CH_3O$ through linear momentum conservation and the sum of its rotational and
vibrational energy content through energy conservation.

Figure 6 shows the energy partitioning of $E_{avl}$ into the translational,
vibrational and rotational degrees of freedom for the two fragments after
excitation of $CH_3ONO$ into the N=O stretching overtones $3_0^1$, $3_0^2$ and $3_0^3$ of
the $S_1$ state (ref. 9). The electronic excitation of NO due to population of
the higher spin-state $\Pi_{3/2}$ (~ 120 $cm^{-1}$ above $\Pi_{1/2}$) amounts to about 50 $cm^{-1}$
and is not included.

## DISCUSSION

We first consider the geometrical properties of the dissociation process (see eqs. 1 - 2 and Fig. 7). Methylnitrite is a planar molecule with respect to its C-O-NO frame in the $S_0$ and $S_1$ state. The $S_1 \leftarrow S_0$ transition dipole moment $\vec{\mu}$ is perpendicular to this plane. The photodissociation creates NO fragments with rotational populations preferentially in large $|M|$ values implying the angular momentum vector $\vec{J}$ to be parallel to $\vec{\mu}$. This fact indicates a dissociation process which proceeds preferentially in the plane of the molecule. The same conclusion is also obtained by an analysis of the $\Lambda$-sublevel populations and the vector correlation between $\vec{J}$ and the fragment recoil velocity vector $\vec{v}$ (ref. 6).
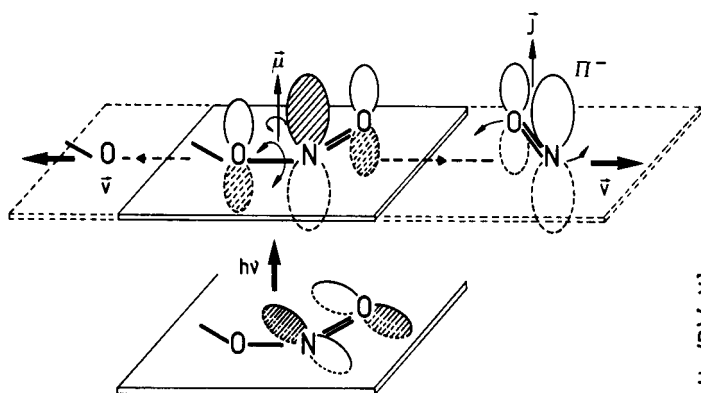


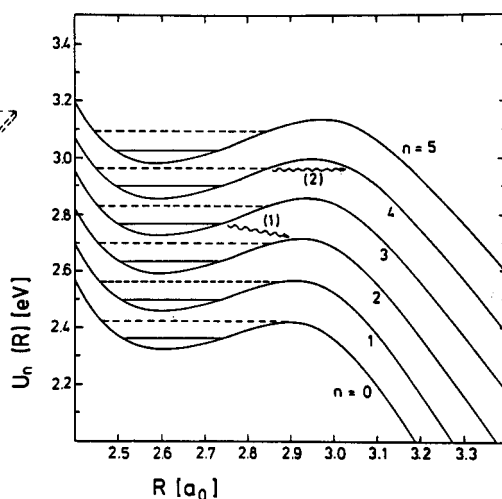Fig. 7. Geometry of the dissociation process which takes place within 200 fs.



Fig. 8. Adiabatic potentials $U(R_{O-N})$ in the region of the local potential well (cf. Fig. 3). The solid and dashed horizontal lines indicate the resonance energies (ref. 10). The arrows indicate the two decay mechanisms, i.e. vibrational predissociation (1) and tunneling (2).

A more subtle picture of the dissociation mechanism is revealed by the $S_1$ potential surface (refs. 5, 10) reproduced in Fig. 3. After absorption of a photon the system is prepared in the Franck-Condon region and starts to e-volve in time. Owing to the shallow well in the PES, an immediate dissociation is prohibited and the activated species is caught for a few vibrational periods ($t_{N=O} \sim 30$ fs) in the potential well. In a second step the decay of the excited molecule is induced by a nonadiabatic and/or a tunneling process. In the first case vibrational-translational coupling causes one quantum of the N=O vibration to be transfered to the dissociation mode.

This situation is illustrated in Fig. 8 which exhibits a series of vibronic PES for $n^* = 0,1,2,3,4,5$. From the $n^*$ PES the decaying species passes to the $n^*-1$ PES and dissociates along this potential producing NO fragments preferentially in the $n^*-1$ vibrational level. Depending on the exit channel interaction further deactivations to $n^*-2$ or $n^*-3$ are also feasible. The tunneling mechanism, on the other hand, provides an adiabatic dissociation pathway along the initial potential curve and gives rise to NO products mainly in $n^*$. The photodissociation of $CH_3ONO$ is thus a nice example of **vibrational predissociation** which involves the special feature of a **strong exit channel interaction**. The final state distribution in the fragments is mainly determined in the exit channel. Even though the activated species performs several vibrations during its lifetime in the potential well, the fragment state distribution is highly non-statistical. A similar behaviour was also found for the related molecule HONO (ref. 13).

The energetics of the dissociation process is summarized in Fig. 6. The reader is refered to ref. 9 for the details of the energy partitioning. 27 - 33 % of the available energy goes into the translational motion of the NO fragment and 12 - 15 % into its rotational degree of freedom. While translation and rotation are only slightly dependent on the overtone excitation, the vibrational energy content of NO is strongly influenced. If the overtone excitation ($\nu_3^n$) of the parent molecule is increased, the additional vibrational energy is channeled exclusively into the NO vibration of the fragment (ref. 3). This high selectivity of vibrational excitation is a consequence of the vibrational predissociation process of $CH_3ONO$ described above.

Recently we have extended our ab initio calculation of the $S_1$-PES of $CH_3ONO$ to include a third dimension. Beside $r_{N=O}$ and $R_{O-N}$ we also varied the angle $O-N=O$. Based on these PES we also performed classical trajectory calculations to obtain the rotational state distribution in NO. The results of these calculations agree well with the experimental findings and thus complete the analysis of the dynamics and state distributions in the $S_1$ dissociation of $CH_3ONO$.

Although the photodissociation of methylnitrite investigated by the LIF technique produces a wealth of data to explore the decay of a polyatomic molecule, a convincing interpretation of the data requires -as in general- a potential energy surface of rather good quality (ref. 18). Such a PES forms the basis for quantum mechanical studies and classical trajectory calculations, which in turn yield the photodissociation dynamics and the state distributions of the products. Fortunately $CH_3ONO$ turned out to be a favorable molecule with respect to this requirement, and the result provided a deep insight into the dynamics of a photodissociation process in a polyatomic molecule, in particular, vibrational predissociation in an excited electronic state.

## Acknowledgement

## REFERENCES

1. H. Okabe, Photochemistry of Small Molecules, Wiley, New York (1978).
2. F. Lahmani, C. Lardeux and D. Solgadi, Chem. Phys. Lett. 102, 523-528 (1983).
3. O. Benoist d'Azy, F. Lahmani, C. Lardeux and D. Solgadi, Chem. Phys. 94, 247-256 (1985).
4. F. Lahmani, C. Lardeux and D. Solgadi, Chem. Phys. Lett. 129, 24-30 (1986).
5. M. Nonella and J.R. Huber, Chem. Phys. Lett. 131, 376-379 (1986).
6. U. Brühlmann, M. Dubs and J.R. Huber, J. Chem. Phys. 86, 1249-1257 (1987).
7. B.A. Keller, P. Felder and J.R. Huber, J. Phys. Chem. 91, 1114-1120 (1987).
8. P. Felder, B.A. Keller and J.R. Huber, Z. Phys. D 6, 185-192 (1987).
9. U. Brühlmann and J.R. Huber, Z. Phys. D 7, 1-8 (1987).
10. S. Hennig, V. Engel, R. Schinke, M. Nonella and J.R. Huber, J. Chem. Phys. 87, 3522-3529 (1987).
11. U. Brühlmann and J.R. Huber, Chem. Phys. Lett. 143, 199-203 (1987).
12. R. Vasudev, R.N. Zare and R.N. Dixon, J. Chem. Phys. 80, 4863-4878 (1984).
13. S. Hennig, A. Untch, R. Schinke, M. Nonella and J.R. Huber, Chem. Phys., submitted
14. M. Dubs, U. Brühlmann and J.R. Huber, J. Chem. Phys. 84, 3106-3119 (1986).
15. C.H. Greene and R.N. Zare, Annu. Rev. Phys. Chem. 33, 119-150 (1982).
16. P. Andresen and E.W. Rothe, J. Chem. Phys. 82, 3634-3640 (1985).
17. R.N. Zare, Mol. Photochem. 4, 1-37 (1972).
18. R. Schinke, V. Engel, S. Hennig, K. Weide and A. Untch, Ber. Bunsenges. f. Phys. Chem. (1988) in press